CHAPTER III.

STRUCTURAL TAILORING AND ACTIVE CONTROL METHODOLOGIES

3.1 Structural Tailoring Technique

As revealed in Chaper 2, the boundary-value problem consists of six differential equations of motion (expressed in terms of the displacements $w_o, \theta_y, \theta_x, u_o, v_o$ and φ), together with the corresponding BCs. Such a set exhibits a complete coupling between the various modes, i.e., primary and secondary warping, vertical and lateral bending, twist and transverse shear.

However, the principal goal of structural tailoring lies in the appropriate selection of fiber orientation so as to produce desired elastic couplings between certain modes. One reason for employing advanced composite materials in flight vehicle design lies in the fact that they permit the use of specific lay-up and fiber orientations so as to induce preferred elastic couplings enhancing the response characteristics. The modified local stiffnesses K_{12}, $K_{13}, K_{14}, K_{24}, K_{43}$ defined in Chapter 2 are responsible for producing the elastic couplings. In this sense, there are two well-known configurations, which are shown in Fig. 3.1 and Fig. 3.2 that create unique and special coupling effects.

The most general governing equations will be specialized to these structural configurations.

<u>3.1.1 Circumferentially Uniform Stiffness (CUS) Configuration</u>

The CUS configuration is characterized by $\theta(y) = \theta(-y)$ shown in Fig. 3.1. A typical CUS configuration can be described e.g. in terms of ply-angle $[\theta]_n$ along the entire circumference of the cross section. In this case, the extensional (A), coupling (B) and bending (D) stiffness coefficients are constant at any point on the cross section, which leads to the modified local stiffness relationship

$$K_{ij}(y) = K_{ij}(-y) \tag{3.1}$$

For the symmetric biconvex cross section as considered herein, the pertinent geometric conditions to be fulfilled along the circumference of the cross section are as follows:

$$\begin{gathered}
\oint x\left(1, y, \frac{dx}{ds}, F_w, a\right)ds = 0, \quad \oint y\left(1, y, \frac{dx}{ds}, F_w, a\right)ds = 0, \\
\oint \frac{dx}{ds}\left(1, \frac{dy}{ds}, F_w, a\right)ds = 0, \quad \oint \frac{dy}{ds}\left(1, \frac{dx}{ds}, F_w, a\right)ds = 0, \qquad (3.2a) \\
\oint \left(F_w, a\right) ds = 0
\end{gathered}$$

Substitution of Eqs. (3.1) and (3.2a) into the definitions of stiffeness coefficients a_{ij}, yields ten independent stiffness coefficients for the CUS configuration. The direct coefficients are a_{11}, a_{22}, a_{33}, a_{44}, a_{55}, a_{66} and a_{77}, while the coupling ones are a_{17}, a_{25} and a_{34}. Proceeding in a similar way with the mass coefficients, one obtains that b_1, b_5, b_{10} and b_{18} are different from zero quantities. Accordingly, in matrix form, the force-displacement equations (2.5.4) reduce to:

$$\begin{Bmatrix} \hat{T}_z \\ M_z \end{Bmatrix} = \begin{bmatrix} a_{11} & a_{17} \\ a_{71} & a_{77} \end{bmatrix} \begin{Bmatrix} w_o' \\ \varphi' \end{Bmatrix} \tag{3.2b}$$

$$\begin{Bmatrix} \hat{M}_y \\ \hat{M}_x \\ Q_x \\ Q_y \\ \hat{B}_w \end{Bmatrix} = \begin{bmatrix} a_{22} & 0 & 0 & a_{25} & 0 \\ 0 & a_{33} & a_{34} & 0 & 0 \\ 0 & a_{43} & a_{44} & 0 & 0 \\ a_{52} & 0 & 0 & a_{55} & 0 \\ 0 & 0 & 0 & 0 & a_{66} \end{bmatrix} \begin{Bmatrix} \theta_y' \\ \theta_x' \\ u_o' + \theta_y \\ v_o' + \theta_x \\ \varphi'' \end{Bmatrix} \tag{3.2c}$$

In this case, the governing system and the associated BCs split exactly into two groups;

i) Extension-Twist vibrations governed by two coupled equations of the sixth order:

$$\begin{aligned} \delta w_o :\quad & a_{11} w_o'' + a_{17}\varphi'' + p_z - T_z^{a\prime} = b_1 \ddot{w}_o, \\ \delta\varphi :\quad & -a_{66}\varphi'''' + a_{71} w_o'' + a_{77}\varphi'' + m_z - B_w^{a\prime\prime} \\ & = (b_4 + b_5)\ddot{\varphi} - (b_{10} + b_{18})\ddot{\varphi}'' \end{aligned} \tag{3.3a}$$

with the associated BCs at $z = 0$:

$$w_o = \varphi = \varphi' = 0 \tag{3.3b}$$

and at $z = L$:

$$\begin{aligned} \delta w_o :\quad & a_{11} w_o' + a_{17}\varphi' = 0, \\ \delta\varphi :\quad & -a_{66}\varphi''' + a_{71} w_o' + a_{77}\varphi' = -(b_{10} + b_{18})\ddot{\varphi}', \\ \delta\varphi' :\quad & a_{66}\varphi'' = 0 \end{aligned} \tag{3.3c}$$

ii) Lateral Bending-Vertical Bending-Transverse Shear vibrations governed by four coupled equations of the eighth order:

$$\begin{aligned} \delta u_o :\quad & a_{43}\theta_x'' + a_{44}(u_o'' + \theta_y') + p_x = b_1 \ddot{u}_o, \\ \delta v_o :\quad & a_{52}\theta_y'' + a_{55}(v_o'' + \theta_x') + p_y = b_1 \ddot{v}_o, \\ \delta\theta_y :\quad & a_{22}\theta_y'' + a_{25}(v_o'' + \theta_x') - a_{43}\theta_x' - a_{44}(u_o' + \theta_y) \end{aligned} \tag{3.4a}$$

$$+ m_y - M_y^{a\prime} = (b_5 + b_{15})\ddot{\theta}_y \,,$$

$$\delta\theta_x : \quad a_{33}\theta_x'' + a_{34}(u_o'' + \theta_y') - a_{52}\theta_y' - a_{55}(v_o' + \theta_x)$$

$$+ m_z - M_x^{a\prime} = (b_4 + b_{14})\ddot{\theta}_x$$

with the associated BCs at $z = 0$:

$$u_o = v_o = \theta_x = \theta_y = 0 \tag{3.4b}$$

and at $z = L$:

$$\begin{aligned} \delta u_o &: \quad a_{43}\theta_x' + a_{44}(u_o' + \theta_y) = 0 \,, \\ \delta v_o &: \quad a_{52}\theta_y' + a_{55}(v_o' + \theta_x) = 0 \,, \\ \delta\theta_y &: \quad a_{22}\theta_y' + a_{25}(v_o' + \theta_x) = 0 \,, \\ \delta\theta_x &: \quad a_{33}\theta_x' + a_{34}(u_o' + \theta_y) = 0 \end{aligned} \tag{3.4c}$$

But the couplings exhibited by CUS configuration are of no interest for the problem at hand, so that the corresponding problem will not be pursued any further.

<u>3.1.2 Circumferentially Asymmetric Stiffness (CAS) Configuration</u>

The CAS configuration is represented by $\theta(y) = -\theta(-y)$ shown in Fig. 3.2. A typical CAS configuration can be described as a combination of $[\theta]_n$ along the upper cross section (defined by y >0) and $[-\theta]_n$ along the bottom cross-section (defined by y <0). In this case, the stiffness coefficients $A_{16}, A_{26}, B, D_{16}$ and D_{26} have constant magnitude around the upper cross section but different signs on the bottom half. As a result, the CAS configuration in terms of modified stiffness terms responsible for this elastic coupling can be characterized by

$$\oint \left(K_{12}, K_{13}, K_{14}, K_{24}, K_{43}\right) ds = 0 \tag{3.5a}$$

In addition to Eq. (3.5a), the geometric conditions expressed by Eqs. (3.2a) have to be considered, as well. Substitution of Eqs. (3.2a) and (3.5a) into the definitions of a_{ij} yields the same direct coefficients as the ones in CUS configuration and a_{14}, a_{37} and a_{56} as the coupling ones. As for the mass terms, by using the same procedure, one obtains that $b_1, b_4, b_5, b_{10}, b_{14}$ and b_{18} are different from zero quantities. Accordingly, force-displacement equations (2.5.4) are reduced to:

$$\begin{Bmatrix} \hat{T}_z \\ \hat{M}_y \\ Q_x \end{Bmatrix} = \begin{bmatrix} a_{11} & 0 & a_{14} \\ 0 & a_{22} & 0 \\ a_{41} & 0 & a_{44} \end{bmatrix} \begin{Bmatrix} w_o' \\ \theta_y' \\ u_o' + \theta_y \end{Bmatrix} \tag{3.5b}$$

$$
\begin{Bmatrix} \hat{M}_x \\ Q_y \\ \hat{B}_w \\ M_z \end{Bmatrix} = \begin{bmatrix} a_{33} & 0 & 0 & a_{37} \\ 0 & a_{55} & a_{56} & 0 \\ 0 & a_{65} & a_{66} & 0 \\ a_{73} & 0 & 0 & a_{77} \end{bmatrix} \begin{Bmatrix} \theta_x' \\ v_o' + \theta_x \\ \varphi'' \\ \varphi' \end{Bmatrix} \tag{3.5c}
$$

Similarly as in the CUS configuration, within the CAS configuration, the extended Hamilton's principle, Eq. (2.6.1) yields two independent boundary-value problems:

i) Twist-Vertical Bending-Vertical Transverse shear motion of the eighth order

$$
\begin{aligned}
&\delta v_o: \quad a_{55}\left(v_o''+\theta_x'\right) + a_{56}\varphi''' + p_y = b_1 \ddot{v}_o \\
&\delta\varphi: \quad \underline{-a_{66}\varphi''''} + a_{77}\varphi'' - a_{56}\left(v_o''' + \theta_x''\right) + a_{73}\theta_x'' + m_z - B_w^{a\,\prime\prime} \\
&\qquad = \left(b_4 + b_5\right)\ddot{\varphi} - \underline{\underline{\left(b_{10} + b_{18}\right)}}\ddot{\varphi}'' \\
&\delta\theta_x: \quad a_{33}\theta_x'' + a_{37}\varphi'' - a_{55}\left(v_o' + \theta_x\right) - \underline{a_{56}\varphi''} - M_x^{a\,\prime} = \underline{\left(b_4 + b_{14}\right)\ddot{\theta}_x}
\end{aligned} \tag{3.6 a-c}
$$

with the associated BCs at $z = 0$:

$$
v_o = 0, \quad \theta_x = 0, \quad \varphi = 0, \quad \underline{\varphi'} = 0 \tag{3.6 d-g}
$$

and at $z = L$:

$$
\begin{aligned}
&\delta v_o: \quad a_{55}\left(v_o' + \theta_x\right) + \underline{a_{56}\varphi''} = 0 \\
&\delta\theta_x: \quad a_{33}\theta_x' + a_{37}\varphi' = 0 \\
&\delta\varphi: \quad \underline{-a_{66}\varphi'''} + a_{77}\varphi' - a_{56}\left(v_o'' + \theta_x'\right) + a_{73}\theta_x' \\
&\qquad = -\underline{\underline{\left(b_{10} + b_{18}\right)}}\ddot{\varphi}' \\
&\delta\varphi': \quad a_{56}\left(v_o' + \theta_x\right) + \underline{a_{66}\varphi''} = 0
\end{aligned} \tag{3.6 h-k}
$$

The terms underscored in Eq. (3.6) by single and double interrupted lines are associated with warping inhibition and warping inertia effect, respectively, whereas the term underscored by a solid line is associated with the rotatory inertia.

As studies on vibration and aeroelastic behavior of wing structures reveal [1, 27, 35], the bending-twist coupling plays a major role, which turns out to be of an exceptional importance towards the enhancement of the response behavior of aircraft wings and helicopter blades. Its beneficial effects, demonstrated within the context of a solid beam model in [1, 27, 47, 48], will be considered herein in the context of a thin-walled beam model.

In view of the importance of cross-coupling stiffness quantities, plots of a_{33}, a_{37}, a_{77}, a_{56} and a_{14} versus ply-angle, θ are portrayed in Fig. 3.3. Based on these plots, a better understanding of the effects played by these stiffnesses quantities on the response behavior can be obtained.

For infinitely rigid in transverse shear beam model, substitution of $a_{55}(v_o''+\theta_x')$ obtained from Eq. (3.6c), once differentiated with respect to z, into Eq. (3.6a) and θ_x replaced by $-v_o'$, leads to the counterparts of Eq. (3.6) as:

$$\delta v_o: \quad a_{33}v_o'''' - a_{37}\varphi''' - p_y - m_z' - M_x^{a}'' = -b_1\ddot{v}_o + \underline{(b_4+b_{14})}\ddot{v}_o''$$

$$\delta\varphi: \quad \underline{-a_{66}\varphi''''} + a_{77}\varphi'' - a_{73}v_o''' + m_z - B_w^{a}'' = (b_4+b_5)\ddot{\varphi} - \underline{(b_{10}+b_{18})}\ddot{\varphi}'' \qquad (3.7\text{ a,b})$$

with the associated BCs $z = 0$:

$$\varphi = \underline{\varphi'} = v_o = v_o' = 0 \qquad (3.7\text{c-f})$$

and at $z = L$:

$$\delta v_o: \quad a_{33}v_o''' = \underline{(b_4+b_{14})}\ddot{v}_o'$$

$$\delta v_o': \quad a_{37}\varphi' - a_{33}v_o'' = 0$$

$$\delta\varphi: \quad \underline{-a_{66}\varphi'''} + a_{77}\varphi' - a_{73}v_o'' = -\underline{(b_{10}+b_{18})}\ddot{\varphi}' \qquad (3.7\text{g-j})$$

$$\underline{\delta\varphi'}: \quad \underline{\varphi'' = 0}$$

From the previously displayed equations, it appears evident that in the case of shear deformable and infinitely rigid in transverse shear thin-walled beams, the governing equations exhibit the same order (namely eight) and the same number of BCs (namely four) has to be prescribed at each edge. A similar characteristic is also valid within the solid beam model [35].

ii) Extension-Lateral Bending-Lateral Transverse shear motion (sixth order governing system)

$$\delta w_o: \quad a_{11}w_o'' + a_{14}(u_o''+\theta_y') + p_z - T_z^{a}' = b_1\ddot{w}_o\,,$$

$$\delta u_o: \quad a_{41}w_o'' + a_{44}(u_o''+\theta_y') + p_x = b_1\ddot{u}_o\,, \qquad (3.8\text{a-c})$$

$$\delta\theta_y: \quad -a_{41}w_o' - a_{44}(u_o'+\theta_y) + a_{22}\theta_y'' + m_y - M_y^{a}' = (b_5+b_{15})\ddot{\theta}_y$$

with the associated BCs at $z = 0$:

$$w_o = u_o = \theta_y = 0 \qquad (3.8\text{ d-f})$$

and at $z = L$:

$$\delta w_o: \quad a_{11}w_o' + a_{14}(u_o'+\theta_y) = 0\,,$$

$$\delta u_o: \quad a_{41} w_o' + a_{44}(u_o' + \theta_y) = 0\,, \tag{3.8 g-i}$$

$$\delta \theta_y: \quad a_{22}\theta_y' = 0$$

The coupling exhibited by the second boundary-value problem is of no interest in this research, so that the problem will not be pursued any further.

<u>3.1.3 Cross-Ply Configuration</u>

Another decoupling occurs in the case of cross-ply TWB structures from the condition of symmetry of the stuctures, which yields $a_{14} = a_{41} = a_{37} = a_{73} = a_{77} = a_{56} = 0$. One is decoupling extension from lateral bending and lateral transverse shear for the Extension-Lateral Bending-Lateral Transverse shear motion in the CAS configuration and the other is the decoupling of twist from vertical bending and vertical transverse shear for the Twist-Vertical Bending-Vertical Transverse shear motion in the CAS configuration.

<u>3.1.4 Transversely-Isotropy Material Structure</u>

In the case of TWBs symmetrically laminated of laminae of transversely-isotropic materials (the plane of isotropy being parallel to the sz surface) assuming that the external loads are distributed along the beam $z-$axis only, an exact decoupling between the transverse bending expressed in terms of v_o and θ_x, lateral bending in terms of u_o and θ_y and the twist, φ is obtained. Herein, we will confine ourselves to the transverse bending (flapping) motion only. Associated with the flapping motion, the corresponding expressions of the 2-D strain measures from Eqs. (2.1.6) and (2.1.7) are

$$\begin{aligned} \varepsilon_{zz}^{o}(s,z,t) &= \theta_x'\, y(s) & \qquad \varepsilon_{zz}^{n}(s,z,t) &= -\theta_x' \frac{dx}{ds} \\ \gamma_{sz}^{o}(s,z,t) &= \left(v_o' + \theta_x\right)\frac{dy}{ds} & \qquad \gamma_{zn}(s,z,t) &= -\left(v_o' + \theta_x\right)\frac{dx}{ds} \end{aligned} \tag{3.8 j-m}$$

In view of the importance of the secondary warping, whose physical significance is discussed by Gjelsvik (1981), and since secondary warping induces transverse bending, this effect is also being considered. Having in view that in this case, $a_{37} = a_{56} = 0$, the equations governing the bending motion are obtained as

$$\begin{aligned} &a_{55}(v_o'' + \theta_x') + p_y = b_1 \ddot{v}_o\,, \\ &a_{33}\theta_x'' - a_{55}(v_o' + \theta_x) + m_z - M_x^{a\prime} = (b_4 + b_{14})\ddot{\theta}_x \end{aligned} \tag{3.9a,b}$$

with the associated BCs at $z = 0$:

$$v_o = \theta_x = 0, \tag{3.9c,d}$$

and with the associated BCs at $z = L$:

$$a_{55}(v_o' + \theta_x) = 0\,, \quad a_{33}\theta_x' = 0 \tag{3.9e,f}$$

Herein a_{33} and a_{55} define the bending and transverse shear stiffness quantities, respectively, which can be expressed as [49]:

$$a_{33} = \oint_C \left[\bar{K}_{11} y^2 + \hat{K}_{11}\left(\frac{dx}{ds}\right)^2 \right] ds,$$

$$a_{55} = \oint_C \left[A_{66}\left(\frac{dy}{ds}\right)^2 + A_{44}\left(\frac{dx}{ds}\right)^2 \right] ds \tag{3.9g,h}$$

where

$$\overline{K}_{11} = A_{11} - \frac{A_{11}^2}{A_{11}}, \quad \hat{K}_{11} = D_{11} \tag{3.9i,j}$$

denote the local reduced stiffness quantities. Herein $A_{ij}\ (i, j = 1,2,6)$ and D_{11} denote local membrane and bending stiffness quantities, respectively, and A_{44} is the local transverse shear stiffness. They are defined in a generic form as

$$\left(A_{ij}, D_{ij}\right) = \sum_{k=1}^{N} \int_{n_{(k-1)}}^{n_{(k)}} C_{ij}^{(k)} (1, n^2)\, dn \tag{3.9 k}$$

where the index k indicates that the quantity in question pertains to the k th layer.

Corresponding to the anisotropy of the transversely-isotropic type featured by the constituent material layers, the elastic coefficients C_{ij} expressed in terms of the engineering constants are [1]

$$C_{11} = \left(E\nu'^2 - E'\right)E/\Delta \qquad C_{12} = -\left(E\nu'^2 + E'\nu\right)E/\Delta$$

$$C_{13} = -\nu'\left(1+\nu\right)EE'/\Delta \qquad C_{33} = -\left(1-\nu^2\right)E'^2/\Delta \tag{3.9 l}$$

$$C_{44} = G' \qquad \frac{C_{11} - C_{12}}{2} = G\left(\equiv \frac{E}{2(1+\nu)}\right)$$

In these expressions, $\Delta = (1+\nu)\left(2E\nu'^2 + E'\nu - E'\right)$; E, ν and E', ν' denote Young's modulus and Poisson's ratio in the plane of isotropy and transverse to the plane of isotropy, respectively, while G' and G denote the transverse shear modulus and in-plane shear modulus, respectively.

For the non-shearable beam model, elimination from Eq. (3.9a) of the quantities $a_{55}(v_o'' + \theta_x')$ obtained from the Eq. (3.9b), operation followed by consideration of Eq. (2.1.2d) stating the absence of transverse shear, results in the equations of motion as

$$-a_{33}v_o'''' + p_y - M_x^{a\,\prime\prime} = b_1\ddot{v}_o - (b_4 + b_{14})\ddot{v}_o'' \tag{3.9 m}$$

with the associated BCs at $z = 0$:

$$v_o = v_o' = 0 \tag{3.9n,o}$$

and with the associated BCs at $z = L$:

$$a_{33}v_o'' = 0 \;, \quad v_o''' = 0 \tag{3.9p,q}$$

3.2 Piezoelectrically Induced Moment Control

The increasing design requirements imposed on a number of important technological structural systems, have led to the development of new active feedback control methodologies. Their implementation is intended, among others, to enhance the vibrational behavior and dynamic response to external excitation and stabilize structures that may be unstable in the absence of control or that may feature only weak structural damping characteristics.

Although the structural/aeroelastic tailoring technique mentioned earlier was proven to be of a great promise in enhancing the static and dynamic response behavior of flight vehicle structures, its efficiency is however limited by the fact that this technique is passive in its nature [3]. Once the ply-angles and ply-sequence of the laminated construction are fixed, the structure can not respond adaptively to the variety of external stimuli imposed upon it during its flight missions. For this reason, as a complementary option, various feedback control schemes can be implemented.

3.2.1 Boundary Moment and Combined Feedback Control Laws

The interest lies in controlling the vibration of the beam by means of a bending moment at the tip. The control law consists of the feedback control concept advocated by Lagnese and Lions [50] and Lagnese [51]. It consists of generation of a moment acting along the boundary of the structure (or part of it).

Such a bending moment control at the wing tip can be generated by incorporating piezoactuators into the structure and using the converse effect featured by these devices. The structures incorporating the capabilities provided by the piezoactuator devices are referred to as intelligent structures. Piezoactuators featuring in-plane isotropic properties, spread over the entire span of the beam and bonded symmetrically on the outer and inner faces of the beam, but activated out-of -phase, generate a bending moment at the beam tip in response to an electric field ξ_3. This permits implementation of a number of control laws which have been proposed in conjunction with boundary moment control as shown in Bailey and Hubbard (1985), Tzou and Zhong (1992) and Librescu *et al* . (1993, 1996). The application of boundary control offers significant advantages, in the sense that the boundary moment remains active in all the modes of vibration, so that boundary control is capable, at least theoretically, of controlling all the infinite modes of vibration. The efficiency of these control laws can be measured in terms of their ability of enhancing the free vibration behavior, reducing the forced vibration to external excitations and preventing resonance.

For the problem at hand, M_x^a is different from zero only if external voltages of opposite signs are applied in the upper and bottom piezoactuator layers (out-of-phase voltage).

Due to the configuration of the piezoactuators which are assumed to be distributed over the entire wing span, the derivatives with respect to z of piezoelectically induced terms in Eq. (3.6c) vanish. This explains why their contributions in the equations of motion is immaterial, but is present only as a nonhomogeneous term in the boundary condition at $z = L$. As a result of implementation of the boundary moment control at the beam tip, Eq. (3.6i), Eq. (3.9f) and Eq. (3.9p) should be replaced respectively by

$$a_{33}\theta_x' + a_{37}\varphi' = M_x^a \tag{3.10a}$$

$$a_{33}\theta_x' = M_x^a \tag{3.10b}$$

$$a_{33}v_o'' = -M_x^a \tag{3.10c}$$

For feedback control, the applied electric field ξ_3 on which the piezoelectrically induced moment depends, may be expressed through a prescribed linear functional relationship with the kinematical response quantities characterizing the wing's response. In order to increase control authority, a combined feedback control law expressed as a combination of angular rotational velocity and acceleration feedback controls can be implemented and is expressed as

$$M_x^a(L,t) = k_V \dot{\theta}_x(L,t) + k_A \ddot{\theta}_x(L,t) \tag{3.11a}$$

where k_V and k_A are the feedback control gains. Replacing Eq. (3.11a) into Eqs. (3.10), the dynamical boundary conditions at $z = L$, can be rewritten in the nondimensional form as

$$\theta_x' = K_V \dot{\theta}_x + K_A \ddot{\theta}_x \tag{3.11b}$$

where $K_V = k_V \bar{\omega} L / a_{33}$ and $K_A = k_A \bar{\omega}^2 L / a_{33}$ are the dimensionless counterparts of the velocity and acceleration feedback gains.

Due to the presence of the bending-twist coupling term a_{37} in Eq. (3.9a), it is clear that the boundary moment can also generate twist. This form of the control law constitutes a generalization of those considered in a number of special cases in Refs. 37, 38 and 52.

Having in view the piezoactuator arrangement for the problem at hand, the boundary control moment M_x^a represented by Eq. (2.5.5b) can be reduced to

$$M_x^a = \oint \sum_{k=1}^{l} \left[\xi_3^{(k)} t^a e_{31}^{(k)} \left[y\left(1 - \frac{A_{12}}{A_{11}}\right) + \frac{dx}{ds}\left(\frac{B_{12}}{A_{11}} - n_k^a\right)\right]\right] ds \tag{3.11c}$$

where t^a is piezoactuator thickness.

In addition, $n_k^a = \frac{1}{2}\left(n_{k^+}^a + n_{k^-}^a\right)$ represents the perpendicular distance from the midplane of the host structure to the center of the piezoactuator.

Since the applied electric field ξ_3 is given by $V(t)/t^a$, the piezoelectrically induced bending moment can be expressed as

$$M_x^a = cV(t) = u(t) \tag{3.11d}$$

where c is a constant dependent upon the mechanical and geometrical properties of piezoactuator and of the main structure and $V(t)$ is the appled input voltage.

3.2.2 Linear Quadratic Controller Design

The control based on LQR consists of finding a control input $\boldsymbol{u}(t)$ which derives the state $\boldsymbol{X}(t)$ to zero in an arbitrary short time. It is assumed that the entire state is available for feedback. The system of equations of motion incorporating the control inputs can be expressed in state-space form as:

$$\dot{\boldsymbol{X}}(t) = \boldsymbol{A}\,\boldsymbol{X}(t) + \boldsymbol{W}\boldsymbol{u}(t) + \boldsymbol{B}\,\boldsymbol{Q}(t) \tag{3.12}$$

where $\boldsymbol{Q}(t)$ is the vector of the arbitrary time-dependent external excitations.

The performance index to be minimized, associated with the linear quadratic regulator problem is often chosen to have the following quadratic form

$$J = \frac{1}{2}\boldsymbol{X}^T(t_f)\boldsymbol{S}\boldsymbol{X}(t_f) + \frac{1}{2}\int_{t_o}^{t_f}\left[\boldsymbol{X}^T\boldsymbol{Z}\,\boldsymbol{X} + \boldsymbol{u}^T\boldsymbol{R}\boldsymbol{u}\right]dt \tag{3.13a}$$

subjected to the constraint given by Eq. (3.12), while $\boldsymbol{S}$ and $\boldsymbol{Z}$ are real symmetric positive semi-definite matrices.

It should be pointed out that the state weighting matrix $\boldsymbol{Z}$ was chosen so that the first term in the cost functional represents the sum of the system kinematic and potential energies [73], or

$$\frac{1}{2}\int_{t_0}^{t_f}\left[\boldsymbol{X}^T\boldsymbol{Z}\boldsymbol{X}\right]dt \;=\; \frac{1}{2}\int_{t_0}^{t_f}\left[\dot{\boldsymbol{q}}^T\boldsymbol{M}\dot{\boldsymbol{q}}+\boldsymbol{q}^T\boldsymbol{K}\boldsymbol{q}\right]dt \tag{3.13b}$$

where $\boldsymbol{q}$ is vector of generalized coordinates, while $\boldsymbol{M}$ is a mass matrix and $\boldsymbol{K}$ is a stiffness matrix.

In addition, $\boldsymbol{R}$ is a real symmetric positive definite control weighting matrix:

$$\boldsymbol{R} = \begin{bmatrix} r_1 & 0 & \cdots & 0 \\ 0 & \ddots & 0 & 0 \\ \vdots & 0 & \ddots & \vdots \\ 0 & 0 & \cdots & r_m \end{bmatrix} \tag{3.13c}$$

It is assumed that $\boldsymbol{X}(t_f)$ is free, $\boldsymbol{X}(t_o)$ is known, and the states and control inputs are not bounded.

Two different situations defining the performance index J will be considered next.

Case I: *External excitation* $\boldsymbol{Q}$ *is included in the Performance Index*

If the external load is assumed to be known a priori, an augmented performance index including the constraint equation, Eq. (3.12) is expressed as

$$J_a = \frac{1}{2}\boldsymbol{X}^T(t_f)\,\boldsymbol{S}\boldsymbol{X}(t_f)+$$

$$\int_{t_o}^{t_f}\left[\frac{1}{2}\left(\boldsymbol{X}^T\boldsymbol{Z}\boldsymbol{X} \;+\; \boldsymbol{u}^T\boldsymbol{R}\boldsymbol{u}\right)+\boldsymbol{k}^T\left(\boldsymbol{A}\,\boldsymbol{X}(t)+\boldsymbol{W}\boldsymbol{u}(t)\;+\;\boldsymbol{B}\,\boldsymbol{Q}(t)-\dot{\boldsymbol{X}}\right)\right]dt \tag{3.14a}$$

where $\boldsymbol{k}(t)$ is Lagrange's multipliers, referred to as the costates.
Reexpressing Eq. (3.14a) as

$$J_a(\boldsymbol{X},\dot{\boldsymbol{X}},\boldsymbol{k};t) = \frac{1}{2}\boldsymbol{X}^T(t_f)\,\boldsymbol{S}\boldsymbol{X}(t_f)+\int_{t_o}^{t_f}\boldsymbol{g}(\boldsymbol{X},\dot{\boldsymbol{X}},\boldsymbol{u},\boldsymbol{k};t)\,dt \tag{3.14b}$$

where

$$\boldsymbol{g}(\boldsymbol{X},\dot{\boldsymbol{X}},\boldsymbol{u},\boldsymbol{k};t) = \frac{1}{2}\left(\boldsymbol{X}^T\boldsymbol{Z}\boldsymbol{X}\;+\;\boldsymbol{u}^T\boldsymbol{R}\boldsymbol{u}\right)+\boldsymbol{k}^T\left(\boldsymbol{A}\,\boldsymbol{X}(t)+\boldsymbol{W}\,\boldsymbol{u}(t)\;+\;\boldsymbol{B}\,\boldsymbol{Q}(t)-\dot{\boldsymbol{X}}\right) \tag{3.14c}$$

the necessary conditions for the optimality can be found by rendering the first variation of Eq. (3.14b) to be zero, which yields

$$\delta J_a = 0 = \delta\boldsymbol{X}^T(t_f)\,\boldsymbol{S}\boldsymbol{X}(t_f)+$$

$$\int_{t_o}^{t_f}\left\{\left(\frac{\partial g}{\partial X}\right)^T\delta X+\left(\frac{\partial g}{\partial \dot{X}}\right)^T\delta\dot{X}+\left(\frac{\partial g}{\partial u}\right)^T\delta u+\left(\frac{\partial g}{\partial k}\right)^T\delta k\right\}dt \tag{3.15}$$

where

$$\frac{\partial g}{\partial X}=Z\,X+A^T k \tag{3.16a}$$

$$\frac{\partial g}{\partial \dot{X}}=-k \tag{3.16b}$$

$$\frac{\partial g}{\partial u}=Ru+W^T k \tag{3.16c}$$

$$\frac{\partial g}{\partial k}=AX+Wu+BQ-\dot{X} \tag{3.16d}$$

Integration by parts of the second term in Eq. (3.15) and making use of Eq. (3.16b) yields

$$\delta J_a=0=\int_{t_o}^{t_f}\left\{\left[\frac{\partial g}{\partial X}-\frac{\partial}{\partial t}\left(\frac{\partial g}{\partial \dot{X}}\right)\right]^T\delta X+\left(\frac{\partial g}{\partial u}\right)^T\delta u+\left(\frac{\partial g}{\partial k}\right)^T\delta k\right\}dt\,+$$

$$k^T(t_o)\delta X(t_o)+\left[X^T(t_f)\,S-k^T(t_f)\right]\delta X(t_f) \tag{3.17}$$

In view of Eqs. (3.16) and (3.17), the necessary conditions for optimality are

$$ZX+A^T k+\dot{k}=\mathbf{0} \tag{3.18a}$$

$$Ru+W^T k=\mathbf{0} \tag{3.18b}$$

$$\dot{X}(t)=A\,X+Wu+B\,Q \tag{3.18c}$$

Since the initial states $X(t_o)$ are known and the final states $X(t_f)$ are assumed free, from Eq. (3.17), one obtains the boundary conditions:

$$\delta X(t_o)=\mathbf{0} \tag{3.19a}$$

$$X^T(t_f)S-k^T(t_f)=\mathbf{0} \tag{3.19b}$$

To find the optimal feedback control law, we express Eqs. (3.18) as

$$\frac{d}{dt}\begin{bmatrix}X\\k\end{bmatrix}=\begin{bmatrix}A & -WR^{-1}W^T\\ -Z & -A^T\end{bmatrix}\begin{bmatrix}X\\k\end{bmatrix}+\begin{bmatrix}BQ\\ \mathbf{0}\end{bmatrix} \tag{3.20}$$

Denote ψ to be the transition matrix of the Eq. (3.20) and let it be partitioned according to the dimensions of $\boldsymbol{X}$ and $\boldsymbol{k}$ as follows:

$$\psi = \begin{bmatrix} \psi_{11} & \psi_{12} \\ \psi_{21} & \psi_{22} \end{bmatrix} \tag{3.21}$$

The solution of the Eq. (3.20) then can be expressed in terms of the final states as [80]

$$\begin{bmatrix} \boldsymbol{X}(t) \\ \boldsymbol{k}(t) \end{bmatrix} = \begin{bmatrix} \psi_{11}(t-t_f) & \psi_{12}(t-t_f) \\ \psi_{21}(t-t_f) & \psi_{22}(t-t_f) \end{bmatrix} \begin{bmatrix} \boldsymbol{X}(t_f) \\ \boldsymbol{k}(t_f) \end{bmatrix} + \int_{t_f}^{t} \begin{bmatrix} \psi_{11}(t-\tau) & \psi_{12}(t-\tau) \\ \psi_{21}(t-\tau) & \psi_{22}(t-\tau) \end{bmatrix} \begin{bmatrix} \boldsymbol{BQ} \\ \boldsymbol{0} \end{bmatrix} dt \tag{3.22}$$

If the boundary condition, Eq. (3.19b) is used, Eq. (3.22) can be rewritten as

$$\boldsymbol{X}(t) = \psi_{11}(t-t_f)\boldsymbol{X}(t_f) + \psi_{12}(t-t_f)\boldsymbol{SX}(t_f) + \int_{t_f}^{t} \psi_{11}(t-\tau)\boldsymbol{BQ}(\tau)\,d\tau \tag{3.23a}$$

$$\boldsymbol{k}(t) = \psi_{21}(t-t_f)\boldsymbol{X}(t_f) + \psi_{22}(t-t_f)\boldsymbol{SX}(t_f) + \int_{t_f}^{t} \psi_{21}(t-\tau)\boldsymbol{BQ}(\tau)\,d\tau \tag{3.23b}$$

Solving for $\boldsymbol{X}(t_f)$ from Eq. (3.23a) and then substituting it into Eq. (3.23b), one obtains the costates $\boldsymbol{k}(t)$ as

$$\boldsymbol{k}(t) = \boldsymbol{P}(t)\boldsymbol{X}(t) + \boldsymbol{d}(t) \tag{3.24a}$$

where

$$\boldsymbol{P}(t) = \left[\psi_{21}(t-t_f) + \psi_{22}(t-t_f)\boldsymbol{S}\right]\left[\psi_{11}(t-t_f) + \psi_{12}(t-t_f)\boldsymbol{S}\right]^{-1} \tag{3.24b}$$

and

$$\boldsymbol{d}(t) = -\boldsymbol{P}(t)\int_{t_f}^{t} \psi_{11}(t-\tau)\boldsymbol{BQ}(\tau)\,d\tau + \int_{t_f}^{t} \psi_{21}(t-\tau)\boldsymbol{BQ}(\tau)\,d\tau \tag{3.24c}$$

By virtue of Eqs. (3.18b) and (3.24a), the linear optimal control law can be expressed as

$$\boldsymbol{u}(t) = -\boldsymbol{R}^{-1}\boldsymbol{W}^{T}\boldsymbol{P}(t)\boldsymbol{X}(t) - \boldsymbol{R}^{-1}\boldsymbol{W}^{T}\boldsymbol{d}(t) \tag{3.25}$$

To determine $\boldsymbol{P}(t)$ and $\boldsymbol{d}(t)$ in Eq. (3.25) we differentiate Eq. (3.24a) with respect to time which yields

$$\dot{\boldsymbol{k}} = \dot{\boldsymbol{P}}\boldsymbol{X} + \boldsymbol{P}\dot{\boldsymbol{X}} + \dot{\boldsymbol{d}} \tag{3.26}$$

By virtue of Eqs. (3.18) and (3.24a) one obtains:

$$\dot{\boldsymbol{k}} = -\boldsymbol{ZX} - \boldsymbol{A}^{T}\left(\boldsymbol{PX} + \boldsymbol{d}\right) \tag{3.27a}$$

$$\dot{\boldsymbol{X}} = \boldsymbol{AX} - \boldsymbol{WR}^{-1}\boldsymbol{W}^{T}\boldsymbol{k} + \boldsymbol{BQ} \tag{3.27b}$$

Replacement Eq. (3.27) into Eq. (3.26) yields

$$\left[\dot{\boldsymbol{P}} + \boldsymbol{Z} + \boldsymbol{A}^T\boldsymbol{P} + \boldsymbol{PA} - \boldsymbol{PW}R^{-1}\boldsymbol{W}^T\boldsymbol{P}\right]\boldsymbol{X} +$$

$$\left[\dot{\boldsymbol{d}} + \boldsymbol{A}^T\boldsymbol{d} - \boldsymbol{PWR}^{-1}\boldsymbol{W}^T\boldsymbol{d} + \boldsymbol{PBQ}\right] = \boldsymbol{0} \tag{3.28}$$

Since the Eq. (3.28) holds for states $\boldsymbol{X}(t)$ at any time $t \quad [t_o, t_f]$, the expressions inside the brackets must be zero, which yields

$$\dot{\boldsymbol{P}} = -\boldsymbol{Z} - \boldsymbol{A}^T\boldsymbol{P} - \boldsymbol{PA} + \boldsymbol{PWR}^{-1}\boldsymbol{W}^T\boldsymbol{P} \tag{3.29a}$$

$$\dot{\boldsymbol{d}} = -(\boldsymbol{A}^T - \boldsymbol{PWR}^{-1}\boldsymbol{W}^T)\boldsymbol{d} - \boldsymbol{PBQ} \tag{3.29b}$$

In addition, according to Eqs. (3.19b) and (3.24a), we have

$$\boldsymbol{SX}(t_f) = \boldsymbol{P}(t_f)\boldsymbol{X}(t_f) + \boldsymbol{d}(t_f) \tag{3.30}$$

By virtue of Eq. (3.30), the terminal conditions of Eqs. (3.29) result as

$$\boldsymbol{P}(t_f) = \boldsymbol{S} \tag{3.31a}$$

$$\boldsymbol{d}(t_f) = \boldsymbol{0} \tag{3.31b}$$

The $\boldsymbol{P}(t)$ and $\boldsymbol{d}(t)$ which appear in the optimal control law described by Eq. (3.25) can be determined from Eqs. (3.29) and (3.31) by solving these equations backward in time. It should be noted that the optimal control law in this case consists of an open-loop control associated with $\boldsymbol{d}(t)$ and a feedback one associated with $\boldsymbol{X}(t)$.

Case II: *External Excitation **Q**(t) is not included in the Performance Index*

In this case, it is assumed that the structure may be subjected to a certain unexpected external transient load. Due to the transient nature of the load, the controller designed on the basis of the unforced structural system might be feasible to be used to suppress the structural vibration. It will be shown later that this simple controller, indeed, is capable of reducing the amplitude of response even in forced as well as in free vibration.

The optimal controller for the controlled system can be obtained in this case as

$$\boldsymbol{u}(t) = -\boldsymbol{R}^{-1}\boldsymbol{W}^T\boldsymbol{P}(t)\boldsymbol{X}(t) \tag{3.32}$$

Within the present work, both Case I and Case II will be considered. In addition, t_o is taken to be zero and $\boldsymbol{S} = \boldsymbol{0}$. In addition, if the terminal time t_f approaches infinity, the Riccati gain matrix $\boldsymbol{P}(t)$ becomes a constant $\boldsymbol{P}_c$ which is the solution to the nonlinear algebraic Riccati equation

$$\boldsymbol{A}^T\boldsymbol{P}_c + \boldsymbol{P}_c\boldsymbol{A} - \boldsymbol{P}_c\boldsymbol{WR}^{-1}\boldsymbol{W}^T\boldsymbol{P}_c + \boldsymbol{Z} = \boldsymbol{0} \tag{3.33}$$

In preceding analysis, there was no limitation on the control input, $\boldsymbol{u}(t)$. But in some situations, the required moment can exceed the moment output capability provided by the actuator. This is due to the limited voltage which can be applied to the piezoactuator. Beyond this limited value, the saturation of piezoactuator occurs. There are several approaches enabling one to handle the problem of the optimal control subjected to satuaration constraint of the controller. Within this study, rather than reducing the feedback gains to accomodate the constraint, the actuator limitation is explicitly addressed in the optimal control algorithm [82, 83]. For unsaturated controller, the optimal controller is obtained same as Eq. (3.32)

$$\boldsymbol{u}(t) = -\boldsymbol{R}^{-1}\boldsymbol{W}^T\boldsymbol{P}(t)\boldsymbol{X}(t) \tag{3.34a}$$

When the saturation limit is met during the period of control, bounds can be placed on the control force as follows:

$$\boldsymbol{u}(t) = \begin{cases} -\boldsymbol{U}_{\mathbf{max}} & \text{for} \quad \boldsymbol{R}^{-1}\boldsymbol{W}^T\boldsymbol{PX}(t) > \boldsymbol{U}_{\mathbf{max}} \\ \boldsymbol{U}_{\mathbf{max}} & \text{for} \quad \boldsymbol{R}^{-1}\boldsymbol{W}^T\boldsymbol{PX}(t) < -\boldsymbol{U}_{\mathbf{max}} \end{cases} \tag{3.34b, c}$$

where $U_{\mathbf{max}}$ is the magnitude of the control input bound for piezoactuator.

In light of Eq. (3.34b, c), the corresponding state equation for the saturated region is expressed

$$\dot{\boldsymbol{X}}(t) = \boldsymbol{AX}(t) \pm \boldsymbol{W}U_{\max} + \boldsymbol{BQ} \tag{3.35}$$

At each sample time, the control input should be checked and while in the saturated region, the appropriate condition Eqs. (3.34b) or (3.34c) is used to modify the control input to pass the algorithm back to the unsaturated region.

3.2.3 Sensor Output Equation

Here one assumes that the piezoelectric elements may be employed concurrently for sensing and actuation [75, 76]. Here we relate the voltage produced by the piezoelectric layer to the strain in the host structure. One also assumes that the host structure features only flapping motion and the piezoelectric patch exhibits anisotropy of a transverse-isotropy type.

For sensing operation, setting ξ_3 equal to zero, the electric displacement results as

$$D_3 = e_{31}\,\varepsilon_{zz} \tag{3.36a}$$

and having in view the expression of the strain measure, ε_{zz} one obtains

$$D_3 = e_{31}\, y(s)\,\theta_x' \tag{3.36b}$$

The charge developed on the sensor can be found through integration of the electric displacement over the corresponding sensor area, or

$$\begin{aligned} q_p(t) &= \int_A D_3\, dA \\ &= \int e_{31}\, y(s)\,\theta_x'\, ds dz \end{aligned} \tag{3.37}$$

The limits of integration in Eq. (3.37) depend on the patch configuration.

The voltage across the piezoelectric sensor can be found by dividing the charge developed in the sensor by the sensor's capacitance, C_p [52]

$$V_p(t) = \frac{q_p(t)}{C_p} \tag{3.38}$$

where C_p depends on the patch area A_p, thickness t^a and the permittivity of the piezoelectric material ξ_{33}^{p}, according to [76]

$$C_p = \frac{\xi_{33}^{p} A_p}{t^a} \tag{3.39}$$

If one considers a single sensor patch, the electric currents required for vibration suppression is determined as

$$\begin{aligned} I &= \frac{dq_p(t)}{dt} \\ &= \int e_{31}\, y(s)\, \dot{\theta}_x{}'\, ds dz \\ &= \int e_{31}\, y(s)\, ds \left[\dot{\theta}_x(z_2) - \dot{\theta}_x(z_1)\right] \end{aligned} \tag{3.40}$$

From the Eq. (3.40) it becomes apparent that the required electric current increases if either the area or thickness of the piezosensor increase relative to the corresponding beam dimensions.

In addition, the power consumption can be obtained as the product of electrical voltage and current as $P = V\ \ I$ [72].

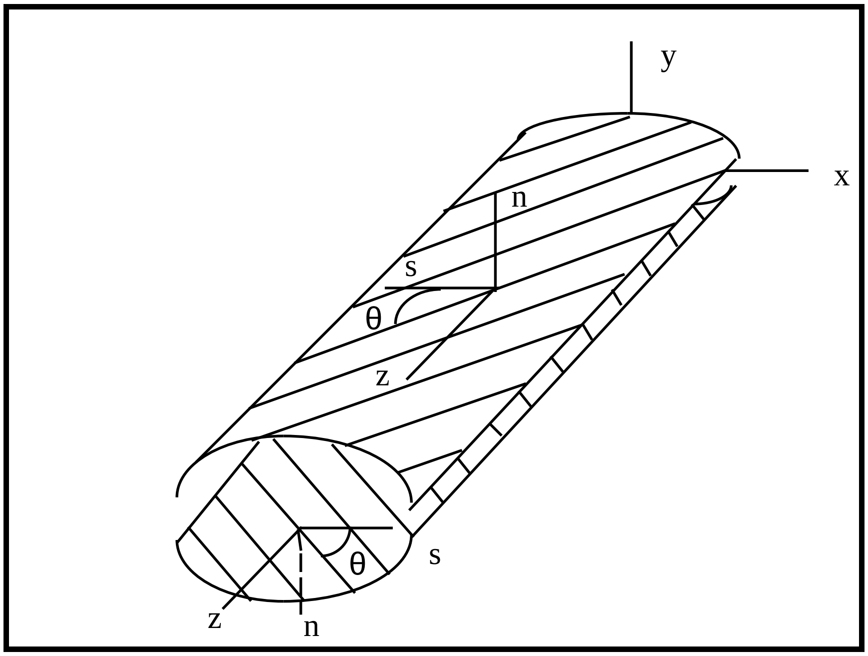

Fig. 3.1 Circumferentially Uniform Stiffness Configuration $\theta(y) = \theta(-y)$.

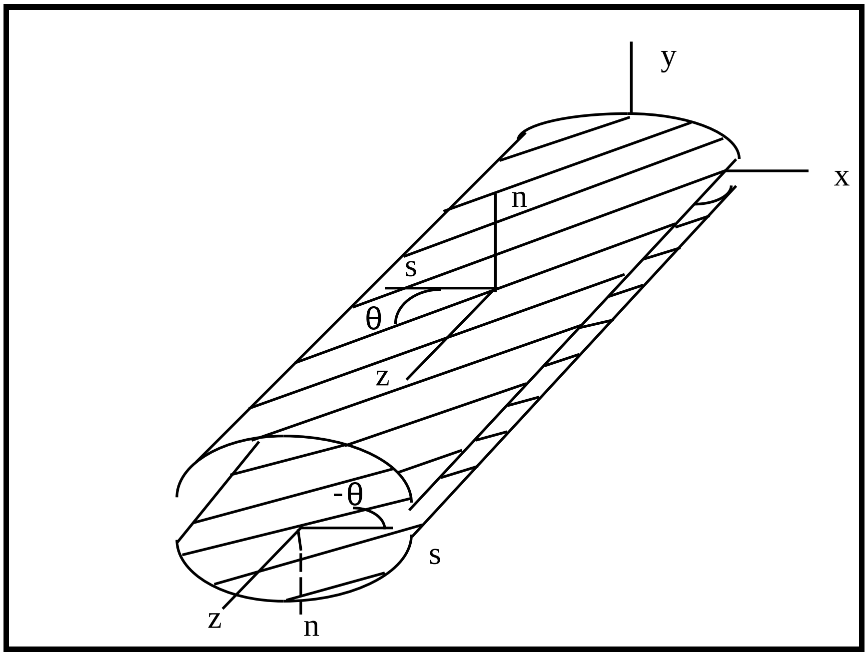

Fig. 3.2 Circumferentially Asymmetric Stiffness Configuration $\theta(y) = -\theta(-y)$.

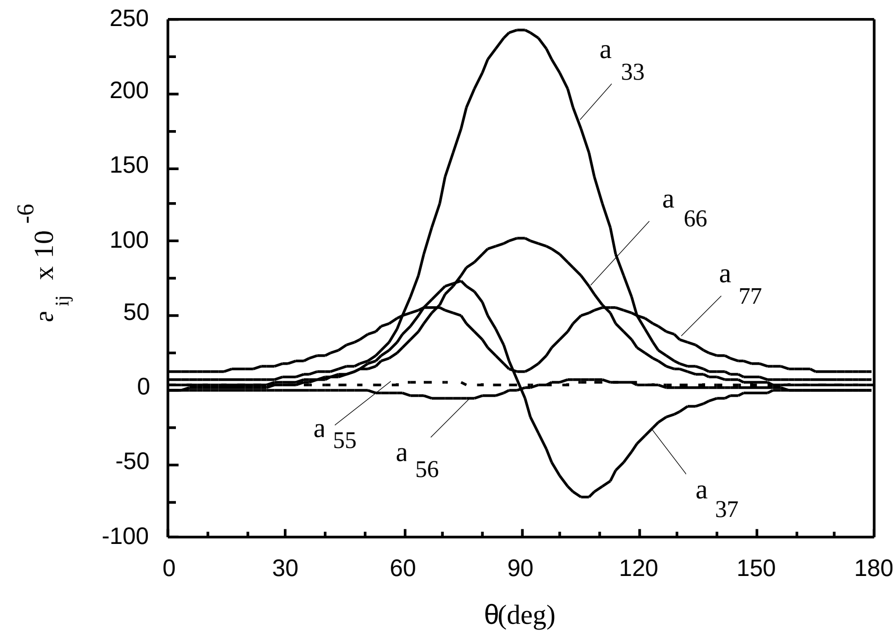

Fig. 3.3 Variation of stiffness quantities with the ply-angle.
Herein

$a_{33}(lb\ \ in^2)$: transverse bending stiffness.
$a_{37}(lb\ \ in^2)$: bending-twist coupling stiffness.
$a_{56}(lb\ \ in^2)$: transverse shear in the y direction-warping coupling stiffness.
$a_{77}(lb\ \ in^2)$: torsional stiffness.
$a_{55}(lb)$: transverse shear stiffness in the y direction.
$a_{66}(lb\ \ in^4)$: warping stiffness.